Sensors and Actuators A 300 (2019) 111657

Contents lists available at ScienceDirect

Sensors and Actuators A: Physical

journal homepage: www.elsevier.com/locate/sna

Laser machined ultrathin microscale platinum thermometers on transparent oxide substrates

Letian Wang[a,*], Zeqing Jin[a], Dongwoo Paeng[b], Yoonsoo Rho[a], Jiangyou Long[a], Matthew Eliceiri[a], YS. Kim[b], Costas P. Grigoropoulos[a,*]

[a] Laser Thermal Lab, Department of Mechanical Engineering, University of California, Berkeley, Berkeley, CA, 94720-1740, USA
[b] Lam Research Corp., 4650 Cushing Pkwy, Fremont, CA, 94538, USA

ARTICLE INFO

Article history:
Received 5 July 2019
Received in revised form
10 September 2019
Accepted 5 October 2019
Available online 7 October 2019

Keywords:
Platinum
Thin film
Temperature sensor
Laser machining
In-Situ

ABSTRACT

Ultrathin microscale platinum resistive thermometers are of key value to transient temperature measurements. Neither transparent oxide substrates nor femtosecond laser patterning have been investigated for the fabrication of Pt thin film thermometers. Here, we have fabricated a laser machined, 50 μm wide and 50 nm thick, serpentine, Pt thin film sensor capable of sensing temperatures up to 650 °C over multiple heating and cooling cycles. Various materials and associated processing conditions were studied, including both sapphire and silica as transparent substrates, alumina and titanium dioxide as adhesion layers, and lastly alumina and silicon dioxide as capping layer. *In-situ* resistance monitoring helps verify the multi-cycle stability of the sensor and guide the optimization. 10 μm sized sensors could be laser-machined, but did not survive multiple heating and cooling cycles. We demonstrate that sensors with amorphous Ge thin layers can also repeatably measure temperatures up to 650 °C. It is anticipated that this sensor can be used for fast, high spatial resolution temperature probing for laser processing of thin films.

1. Introduction

Transient temperature measurement techniques come mainly in three categories [1]: electrical, optical and contact. Compared to the contact method, optical and electrical methods can provide a shorter response time. Resistive electrical sensing requires minimal instrumentation or prior knowledge of the material properties compared to optical methods. Furthermore, it is not affected by the surface conditions of the probed system, which is ideal both for the development of new thermal processes and integration with mass-produced devices.

High spatial resolution and ultrathin thin-film resistive thermometry is critical to various transient temperature probing tasks. Pt is a favorable high-temperature functional material as it is chemically inert and has a linearly temperature dependent resistivity. High spatial resolution Pt thermometers have been widely used in MEMS thermometers [2–5], heaters [6,7] and micro-reactors [8,9]. An ultrathin sensor structure contains less mass, leading to shorter response time and minimum thermal interference with the probed system. Beyond MEMS applications, laser based additive manufacturing's commercial adoption necessitates research and understanding of this transient process. Highly localized temperature data will enable monitoring of local melting and solidifying processes, critical for process control of laser-based manufacturing [10–12]. As laser sintering resolution is pushed to the micron-scale [13], measurement of relatively local temperature becomes increasingly challenging. In addition, recent advancement in pulsed laser processing [14–20] requires the thickness of the sensor to be thin enough for a nanosecond response time.

Since previous studies focus on MEMS applications in silicon [4,21], resistive sensors on transparent oxides are rarely investigated. Most biological and chemical microfluidic chips are built on quartz and glasses, for which the thermometer applications should be addressed. More importantly, laser-based manufacturing and processing of nanomaterials happens mainly on dielectric substrates including ceramics and glasses due to their low optical absorptivity and high thermal stability. Besides these features, transparency is also of interest as it provides possibility to study the laser beam's thermal and optical effects separately by delivering the laser light from the bottom or the top of the substrate. Two typical dielectric substrates, sapphire [22] and silica were targeted

* Corresponding authors.
E-mail addresses: letianwang@berkeley.edu (L. Wang), cgrigoro@berkeley.edu (C.P. Grigoropoulos).

https://doi.org/10.1016/j.sna.2019.111657
0924-4247/

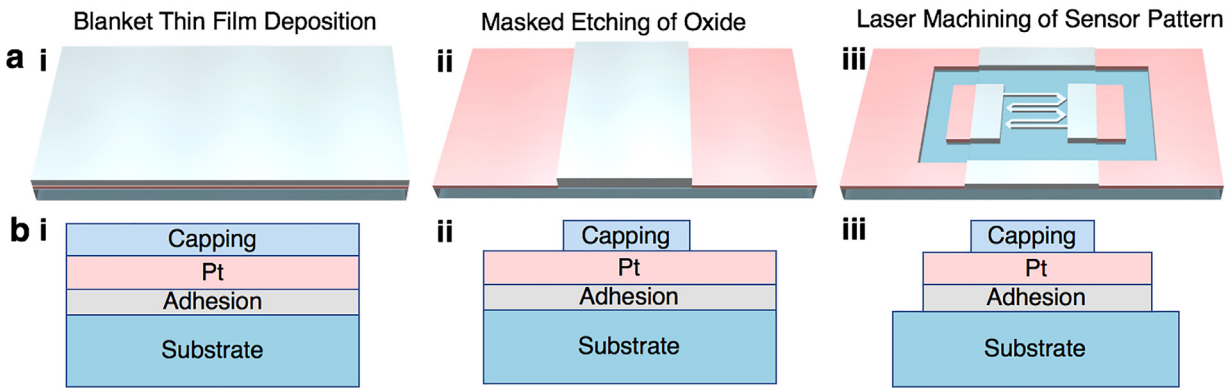

Fig. 1. Fabrication process flow for Pt thin film sensors without additional target layers. (a) Blanket deposition of adhesion, Pt and capping layers. (b) Masked etching of capping layer to expose Pt layer for electrical contact. (c) Laser micromachining of sensing pattern and electrical contact. In each panel, figure i and ii are 3D perspective and cross-sectional views respectively. "Capping" layer stands for either bare oxide capping or the case with amorphous Ge on top of oxide. (For interpretation of references to the colors in this figure, the readers are referred to the web version of this article).

Table 1
Thermal conductivity and expansion coefficient for materials used in the study.

Material	Thermal Conductivity (W/mK)	Thermal Expansion (10^{-6} m/(m K))
Pt	71 [23]	8.8 [24]
Si	130 [23]	2.6 [24]
Fused Silica	1.5 [23]	0.55 [25]
Sapphire	23.1 [23]	5.3 [25]
Alumina	18 [23]	8.1 [25]
TiO_2	4.8-11.8 [26]	8.2-11.8 [26]

for testing based on their distinctly different thermal conductivities and thermal expansion coefficients (Table 1).

Femtosecond laser machining is a strong candidate for fabricating high-resolution thin film microsensors. The high-resolution sensors are conventionally fabricated with costy photolithograph. The removal of Pt layer is also challenging as the inert nature of Platinum makes reactive ion etching time consuming. On the other hand, lift-off of the Pt film on top of the resist will involve more chemicals, more steps and wet-processing. Furthermore, the application of photoresist will reduce the adhesion layer's adhesion to the Pt layer, thus leading to unstable thermal performance. Femtosecond laser machining has been a high throughput and cost-effective industry approach for manufacturing Pt-based resistive temperature detector (RTD) elements [27]. Recent studies indicate that it is possible to machine sub-micron scale features on metal films [28]. Due to the maskless, non-vacuum, environmentally friendly, and cost-effective fabrication nature, femtosecond laser machining can be applied to large scale glass, ceramic, and even flexible substrates [29]. Furthermore, on-demand laser writing offers an agile manufacturing approach, capable of patterning [30], fine-tuning resistance, and arranging multiple sensors for mapping temperature distributions [31].

Here, we present the successful fabrication of a stable, 50 nm thick Pt high temperature sensor on transparent oxide substrates. With femtosecond laser machining, a critical dimension of 5 μm and a total size of 50 μm is achieved. To ensure stability upon repeated heating, we carried out a comprehensive study on the material selection and associated processes for different substrates, adhesion layers, insulation layers and top layers. *In-situ* resistance monitoring (Firebaugh et al. [34]) has characterized the degradation and informed sensor optimization. Though ultrathin microscale sensors are applicable to various applications, the parameters of the current sensor are optimized towards probing laser induced transient temperature fields. As a consequence, the Pt thickness must be larger than 50 nm to provide enough mechanical robustness against pulsed laser induced impacts. 50 nm Pt films have a thermal response time below 500 ps, sufficient for probing transient temperature change induced by pulsed lasers. The obtained 50 μm spatial size is limited by the resolution of femtosecond laser machining degradation caused by subsequent defects. Nevertheless, it is consistent with powder size (30–50 μm) and focused laser beam size (80 μm) in metal laser selective printing [32]. The resulting fabricated sensor was determined to have the specifications required for probing transient temperature change induced by pulsed laser irradiation.

2. Sensor fabrication

The sensor's fabrication flow is demonstrated in Fig. 1, which takes mainly three steps, blanket thin film deposition, shadow masked wet etching of capping layer and lastly the laser machining of sensor patterns. Depending on what type of temperature sensing is required, there could an additional target layer on top of the capping layer, whose temperature is of interest upon specific thermal processing. Below we will review the major consideration during the fabrication process.

The sensor fabrication starts with blanket thin film deposition of an adhesion layer, a Pt layer and a capping layer on the selected substrates (Fig.1a). As described in the introduction, sapphire and fused silica were chosen as substrates, as Sapphire [35] has been reported to form epitaxial interfaces and strong adhesion with the Pt layer after annealing. For fused silica, however, adhesion to Pt is poor due to mismatched crystalline structure and thermal expansion coefficient (Table 1). Conventional Ti/ Cr metal adhesion layers suffer from oxide diffusion [36] in high-temperature annealing. Al_2O_3 [37,38] and TiO_2 [38,39] has been reported to show good adhesion with both Pt and oxide substrates without diffusion. Hence, a 7 nm thick Al_2O_3 layer and a 15 nm thick TiO_2 layer are deposited as adhesion layer on silica substrates with Atomic Layer Deposition (ALD, Cambridge) at 300 °C for 50 min. The sample is then electron-beam evaporated (CHA solutions) with 50 nm thick Pt film under 10^{-6} Torr. To test the adhesion, we used the tape adhesion test and found that the combination of Pt-sapphire survived multiple tape peelings, while the combination of Pt-Al_2O_3-silica and Pt-TiO_2-silica survived one cycle, and the Pt-silica and Pt-oxide-Si were immediately destroyed. From Table 2, before capping the oxide, properly adhered samples (2–4) have a similar sheet resistance of 3.45 while Pt/Oxide combinations (1 and 5) have 10% higher resistance probably due to the poor adhesion.

The deposition of the capping layers reduced Pt sheet resistance by inducing additional annealing. The capping layer is important for

Table 2
Sheet resistance of Pt film on different substrates before and after capping.

No	Substrates	Adhesion Layers	Before Capping		Capping Oxide	
			Sheet Resistance (Ω/sq)	Specific resistance (μΩ·cm)	Sheet resistance (Ω/sq)	Specific resistance (μΩ·cm)
1	Silica	–	3.81	19.05	2.58	12.9
2	Silica	TiO_2	3.51	17.55	3.42	17.1
3	Silica	Al_2O_3	3.46	17.3	2.67	13.35
4	Sapphire	–	3.37	16.85	2.70	13.5
5	Silicon with oxide	–	3.82	19.1	2.93	14.65

temperature sensing as it prevents electrical shortages, chemical diffusion or mechanical damage to the underlying Pt layer. All the samples from the above processes are capped with 45 nm PECVD oxide at 350 °C for 15 min. After capping the oxide, the sheet resistances dropped significantly which we posit is due to the annealing accompanied by the deposition process [36]. The additional thermal processing will anneal the sample to ameliorate defects and increase the grain size [40]. The specific resistance of Pt thin film is as high as 19.1 μΩ·cm (before capping) and as low as 12.9 μΩ·cm (after capping). Though larger than 10.7 μΩ·cm from the bulk Pt [41], it agrees well with the results obtained on 60 nm Pt film with 18.7 μΩ·cm (before) and 12.6–13.3 μΩ·cm (after annealing at 300 °C) by Schmid et al. [42]. Similar results are also obtained for 180 nm Pt film with 18 μΩ·cm (before) and14.5 μΩ·cm (after annealing 700 °C) by Resnik et al. [5]. For TiO_2, the resistance is not reduced significantly which could be due to the unique structural changes of TiO_2. [34,43] The effect of different capping layer thicknesses and processing times are investigated and discussed in the results section.

In some samples of section. 3.5, additional Ge thin films are deposited on top of the capping layer to demonstrate the sensor's application. In some applications, Pt sensors are required to sense the temperature of other thin films that are being thermally processed. Hence it is important to show that Pt can function properly with additional layers on top of its capping layer. Germanium is an important high mobility and functional electronic material [44] and has been the subject of various thermal annealing studies [45,46]. Therefore, Ge is selected as the target material and its melting point is high enough to withstand 900 °C, which is valid for most thermal processing applications. Electron beam evaporation is applied to deposit thin amorphous germanium films to avoid ion bombardments. The Ge layer is not shown on Fig.1, but it behave the same as the capping layer for step 2 and 3.

After all the layers are deposited, the sample is shadow-masked in the center and etched with peroxide (for the samples with Ge layers) and buffered HF to expose part of the Pt layer for electrical contact (Fig. 1b). After masked etching, a femtosecond pulsed laser (800 nm, 1 kHz, Spitfire, Spectra-physics) is used to machine the serpentine sensor and the electrical contact pads (Fig. 1c). We eliminated the additional metal contact deposition to simplify the process and reduce degradation [47]. High-temperature compatible silver-paste (Ted Pella) serves as contact forming agent between the Pt contact pad and the lead wires. However, for probing laser processing, high resistance should be introduced in the sensing unit to ensure negligible error caused by the contact pad. The serpentine sensor structure is designed and fabricated with a femtosecond laser under a 100X objective lens (Fig.2b i). Most samples studied are machined to a 4 mm scale, and in one-section the sample sizes are reduced to 10 μm. For the smaller, 10 μm sensor, the side roughness in high-resolution machining is significant compared to the line width, which is caused by the non-uniform film quality and the stage motion stability. Further optimization might be obtained through prolonged annealing after machining.

As the samples are properly insulated from oxidation, a tube furnace (Lindberg) is used to heat the sample in ambient air conditions for the calibration of Temperature Coefficient of Resistance (TCR). A separate K-type high-temperature compatible thermocouple is inserted into the tube close to the sample. The temperature and voltage change on the resistor are recorded *in-situ* through digital data logger (HIOKI LR8431). We carried out heating and cooling cycles to calibrate the TCRs of the sample using a maximum ramping rate 50 °C /min. The sensor's TCRs are distributed near 2500–2800 ppm/K, which agree with results from the 200 nm Pt thin film [48] annealed between 250–450 °C. The *in-situ* study helps to monitor the failure and the hysteresis of the sensor under the high-temperature annealing.

3. Results

3.1. Substrate effect on thermal stability

Pt sensors on sapphire substrates demonstrate better thermal cycling stability compared to those on silica + TiO_2 and silica + Al_2O_3. In Fig. 3, the Pt sensor on sapphire has demonstrated almost identical heating and cooling TCR in 2 cycles up to 700 °C (Fig. 3a–b). We attribute such stability to the epitaxial crystallinity match between Pt and sapphire [35], which is consistent with the adhesion tests. The Silica + TiO_2 combination shows significant hysteresis effects resembling the results from Pt on the Ti adhesion layer [34]. The hysteresis is also increased after the 2nd heating and cooling cycle. (Fig. 3c ii)). No chemical diffusion is observed for TiO_2 under Pt up to 800 °C [39] and agglomeration is considered to be the main degradation mechanism, which has been proved in previous studies [34]. As it is later addressed on other substrates, a detailed investigation is not pursued. Upon further consideration of the TiO_2 absorptivity [49] and its semiconducting behavior [50], this material is not further pursued as the adhesion layer for Pt on silica. For silica + Al_2O_3, no hysteresis is seen in the cycling but significant failure is observed in the 2nd cycle. The failure is later suppressed with longer annealing time (Fig. 4) of the substrate and adhesion layer and its cause is also discussed in the next section. Identical experiments were carried out on Si-SiO_2 substrates and a similar hysteresis was observed, which is considered also the agglomeration but not investigated with more details. In summary, the sapphire and silica + Al_2O_3 substrates show promise for high-temperature sensing.

3.2. Capping layer effects on the thermal stability

The effect of capping layer on the thermal stabilities is studied on silica substrates. Low cost and low thermal conductivity make silica an important substrate for laser processing. The aforementioned initial attempt with the silica + Al_2O_3 substrate, however, only survived the 1st cycle of heating. Based on the possible sources of degradation, two improvements are investigated, namely depositing a thick oxide or an additional thin ALD step. Firstly, a thicker capping oxide layer offers stronger surface constraints to reduce agglomeration and deformation. Experimental results (Fig.4a) show 110 nm capping layer exhibited reduced hysteresis over multiple annealing cycles and achieved repeatable

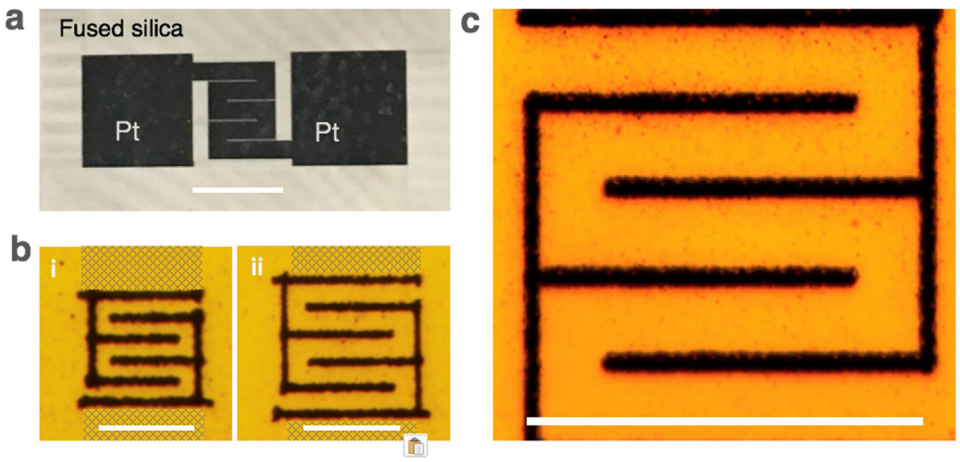

Fig. 2. Femtosecond laser machining of the Pt sensor. (**a**) overview of the femtosecond laser machined large scale sensor with 4 mm size. (b) microscale sensor pattern with (i)10 μm, (ii)15 μm sized serpentine sensor pattern. (c) 50 μm sized sensor. The scan speed is 0.1 mm/s. The separation region between contact pads are not machined in the image b–c to avoid residual built-up, but they are noted as dashed lines. The scale bars in a–c are 5 mm, 10 μm and 50 μm, respectively.

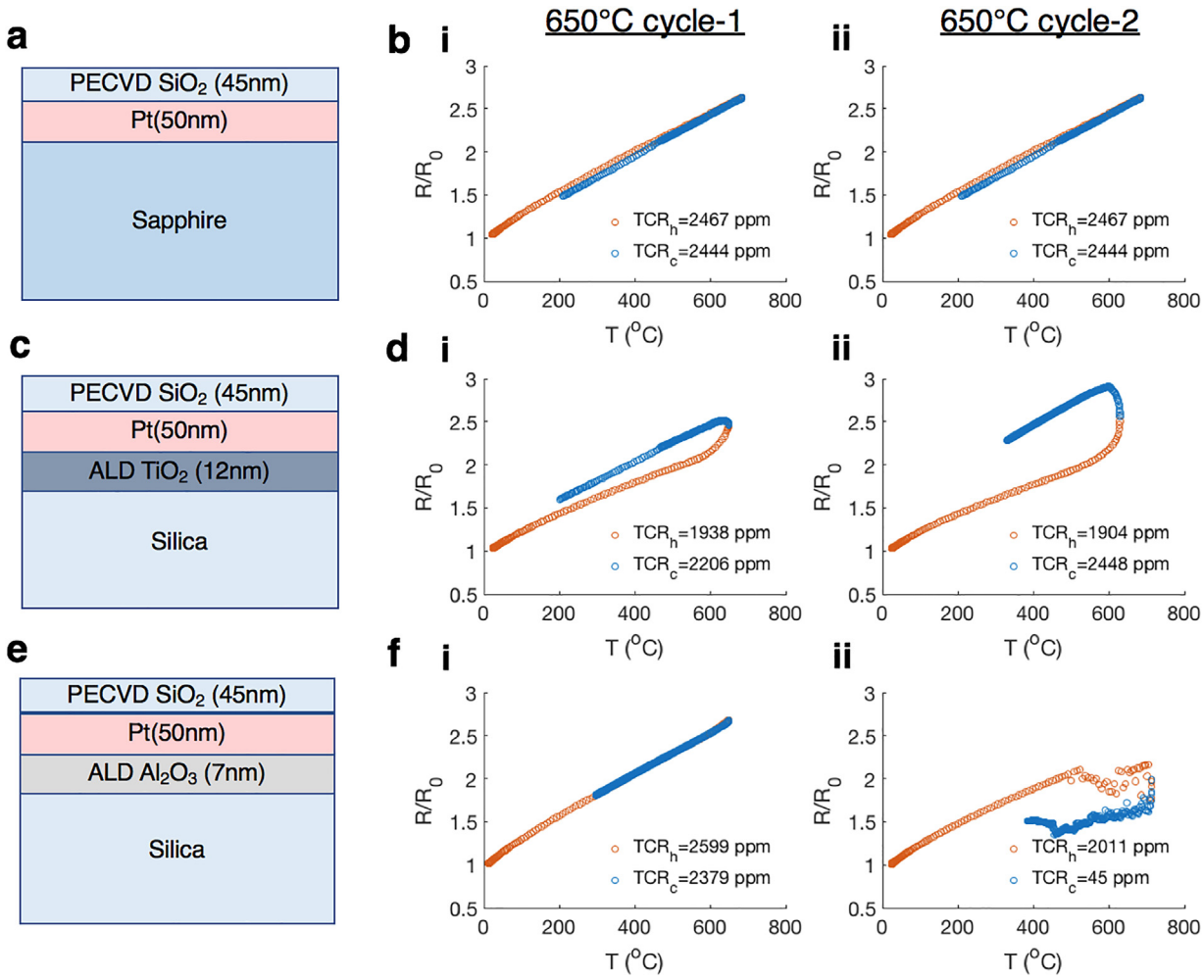

Fig. 3. Temperature dependent resistance calibration of Pt sensor on sapphire, silica + TiO_2 and silica + Al_2O_3 substrates. (**a**) schematics of the sensor on a sapphire substrate and (b) its resistance history upon 2 cycles. (i-ii) of heating and cooling at 650 °C. (**c**) Silica + TiO_2 substrates and (**d**) its resistance history. (**d**) Silica + Al_2O_3 substrates and (**e**) its resistance history. All the samples are capped with 45 nm PECVD oxides. The heating and cooling curves are labeled with red and blue, and the TCRs are plotted in the legends. (For interpretation of the references to colour in this figure legend, the reader is referred to the web version of this article.)

results (Fig. 4a–b). Secondly, given the good adhesion between Pt with Al_2O_3, symmetrically placing Al_2O_3 interfacial layers on both sides of the Pt layer is anticipated to improve stability. A 7 nm thick ALD Al_2O_3 layer is deposited on top of Pt thin films and repeatable results are obtained as well (Fig. 4c–d). The successful results show that neither thickness nor the choice of capping material is the critical requirement for repeatable thermal results. Alternatively, since both PECVD 110 nm oxide(35 min) and ALD Al_2O_3 (40 min)

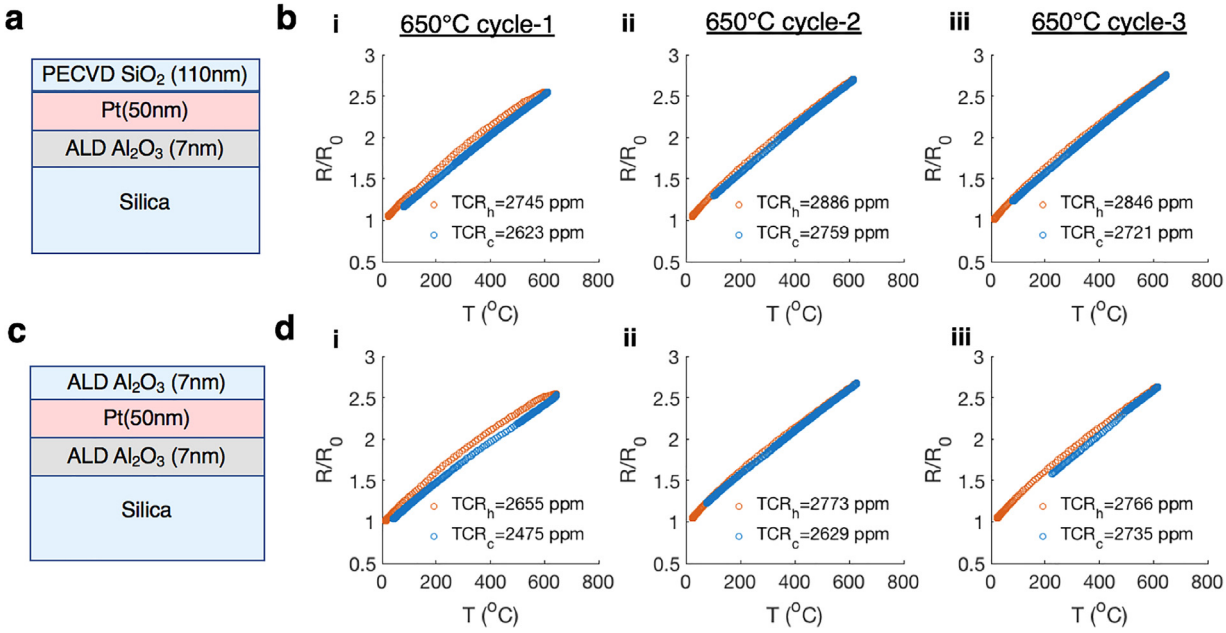

Fig. 4. Temperature dependent resistance calibration of silica + Al_2O_3 substrate capped with different capping layers. (**a**) schematics of structures with PECVD 110 nm SiO_2 as capping layer and (**b**) the resistance history upon three cycles of heating and cooling at 650 °C labeled with (i-iii). (**c**) schematics of structures with ALD 7 nm Al_2O_3 as capping layer and (**d**) the resistance history upon the same processing as (**b**).

involve at least two times longer thermal annealing than PECVD 45 nm oxide(17 min), the effective annealing time is considered to be the main factor for stability. With an increased number of heating cycles, the hysteresis effect is reduced, leading to less difference in TCRs for heating and cooling. Further, the overall value of TCRs increases, agreeing with the literature [48]. Insufficient annealing time means larger residual stress [51] inside Pt and between layers, which contribute to the stronger hysteresis manifested in Fig. 3fii. However, the failure of Fig. 3e–f indicates that the stress is released properly only when constant temperature annealing is implemented before any fast ramping heating. Otherwise, faster ramping and cooling does not help and may lead to sensor failure.

3.3. High temperature sensing

Ability to sense temperature as high as possible is desired as laser processing of semiconductor thin films can easily reach 900 °C [52,53]. We first confirm the Pt sensor on sapphire substrate survived three cycles of heating and cooling at 650 °C (Fig.5). For another identical sample, we ramped the temperature to 900 °C after one cycle of 650 °C. A significant deviation is generated at around 800 °C and similar hysteresis as silica + TiO_2 is observed afterward. An extreme hysteresis is generated at the 3rd cycle, indicating the failure of the sensor. Therefore we conclude that agglomeration is generated at high annealing temperature above 800 °C. The sensor's maximum temperature range for steady-state measurement is between 650–800 °C.

3.4. Sensor with different sizes

Miniature sensors are ultimately required for probing microdevices or focused laser induced temperature fields. To study the minimum sensor size, we designed the sample to 200 μm, 50 μm and 15 μm sizes. All the sensors are manufactured on silica-alumina substrates and capped with an ALD alumina thin layer. The measured TCR and drifting characteristics during repeated heating and cooling cycles are listed in Table 3. It is clear the previous annealing condition for 6 mm sensor (Fig. 4c) is not enough to stabilize the 200um sensor, leading to hysteresis. Fortunately, the TCR is stabilized and the hysteresis is removed upon more heating and cooling cycles. For the 50um sensor, the TCR is not stabilized upon the 3rd cycle and hysteresis is generated. Smaller size induced stress concentration increased the requirement of stress release and annealing. Annealing before laser machining is shown to provide a proper solution and is discussed in the next section.

Table 3
TCR measurement for the sensors with different sizes.

Size(μm)	Cycle	TCR(h/c) (ppm/K)	Hysteresis
200	1	2403/2083	Yes
200	2	2614/2197	No
200	3	2507/2091	No
50	1	2102/2093	No
50	2	2298/2189	No
50	3	2303/1993	Yes
15	1	1703/1203	Yes

h stands for heating, c stands for cooling.

When we machine 15 μm sized sensors, significant electrical shorting as well as diverging heating and cooling curves were observed, where the resistance dropped dramatically, returned to normal, and fell again afterwards. Microscopic images indicate thin-film flaking (Fig.6) is the cause of the shorting effects. Since the flake is easily detached after vibration, we note the sensor completely lost conductance after being disconnected from the measurement apparatus. The laser ablation induced shock wave delamination effects [54,55] reduced the Pt stripe's mechanical integrity and adhesion to the substrate. When the size of the sensor is reduced to 15 μm, such effects will be critical and lead again to sensor failure. Similar to the above problem, annealing before laser machining and longer annealing are believed to further reduce the minimum sensor size.

3.5. Microscale sensor with top layer

We investigated the thermal stability of the sensor with an amorphous Ge layer deposited on top, and the results are listed

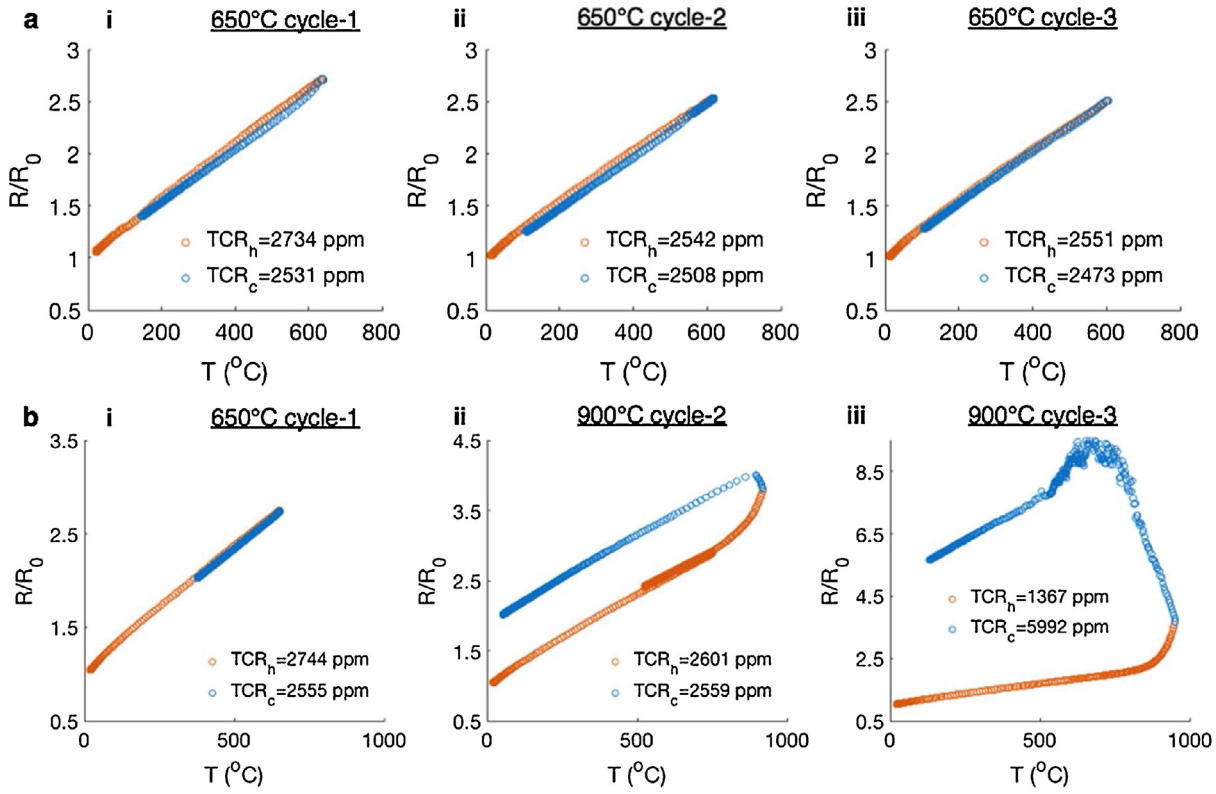

Fig. 5. Temperature dependent resistance calibration of Pt sensor on sapphire substrates with different maximum temperatures. (a) 650 °C (b) 900 °C with 1–3 cycles labeled with (i-iii).

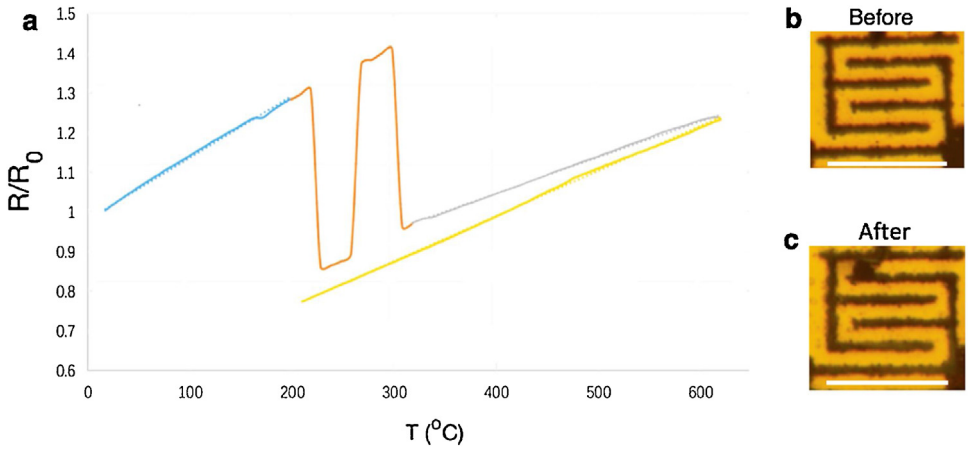

Fig. 6. Failure of 15 μm sized Pt sensor under one single heating and cooling cycle. (**a**) temperature dependent resistance measurement during 1st cycle heating and cooling. "Blue", "orange" and "grey" stand for heating process and "yellow" stands for cooling. Optical bright-field image of the sample (**b**) before 1st cycle testing and (**c**) after 1st cycle testing. The scale bars in (b–c) are 15 μm. (For interpretation of the references to colour in this figure legend, the reader is referred to the web version of this article.)

Table 4
TCR measurement for the sensors with Ge as the top layer.

Size(μm)	Cycle	TCR(h/c) (ppm/K)	Machine-Anneal sequence	Hysteresis
200	2nd	2510/2634	MA	No
200	3rd	2602/2621	MA	No
50	2nd	2198/1667	MA	Yes
50	3rd	2093/2406	MA	Yes
50	2nd	2513/2399	AM	No
50	3rd	2507/2523	AM	No

in Table 4. The original sensor is capped with PECVD 45 nm thick oxide and hence no hysteresis is anticipated for the 1st cycle. However, a sensor with an amorphous Ge layer presented significant TCR hysteresis in the 1st cycle. The Ge layer introduced additional stresses during deposition and also restricted the stress release during the laser machining process. However, at the 2nd and 3rd cycle, the TCR stabilized without any hysteresis as the stress is properly released. For 50 μm size sensors, the sensor obtained just slight improvement at the 2nd and 3rd cycle. We presume that the focused laser ablation generates sufficiently high stresses, and once these stresses are coupled with top layer confinement they cause irreversible degradation. As a solution, we propose annealing the sample before laser machining to release the stress and reduce the defects. A thermally stable 50 μm sensor with a top layer is successfully demonstrated.

4. Conclusion

We have developed fabrication processes for a stable 50 nm thick microscale Pt thermometer on transparent substrates. The silica substrate with an ultrathin TiO_2 adhesion layer gives an increasing hysteresis response of the TCR with repeated heating and cooling. Sapphire and silica with alumina adhesion provide repeatable TCRs for cycling tests at up to 650 °C, which fails at 900 °C. Laser machined sensors reach a minimum size of 10 μm. However, under heating test, 15 μm size thermometers will fail with irreversible film flaking. Only sensors of at least 50 μm survived repeated heating and cooling. Annealing before laser machining resolved the hysteresis problem induced by deposition of an additional Ge thin film and provide a strategy for further reduction of sensor size. A 50um sensor with a thin Ge layer on top shows repeatable TCR performance and is ready for measurement of temperature change upon laser processing.

Acknowledgment

The nanofabrication and SEM were carried out at the Marvell Nanofabrication Laboratory and the California Institute of Quantitative Bioscience (QB3) of UC Berkeley. The authors would like to thank Chris Zhao from in Novellution Technologies, Inc. for helpful discussion on the sample fabrication. Letian Wang received financial support from Lam Research Fellowship. The work received financial support from NSF CMMI funding No. 1363392.

References

[1] D.L. Blackburn, Temperature measurements of semiconductor devices - a review, Twent. Annu. IEEE Semicond. Therm. Meas. Manag. Symp 20 (2004) 70–80, http://dx.doi.org/10.1109/STHERM.2004.1291304 (IEEE Cat. No.04CH37545).
[2] L. Zhu, A. Fiorino, D. Thompson, R. Mittapally, E. Meyhofer, P. Reddy, Near-field photonic cooling through control of the chemical potential of photons, Nature 566 (2019) 239.
[3] D. Thompson, L. Zhu, R. Mittapally, S. Sadat, Z. Xing, P. McArdle, M.M. Qazilbash, P. Reddy, E. Meyhofer, Hundred-fold enhancement in far-field radiative heat transfer over the blackbody limit, Nature 561 (2018) 216.
[4] L. Cui, W. Jeong, S. Hur, M. Matt, J.C. Klöckner, F. Pauly, P. Nielaba, J.C. Cuevas, E. Meyhofer, P. Reddy, Quantized thermal transport in single-atom junctions, Science 355 (2017), 1192 LP – 1195 http://science.sciencemag.org/content/355/6330/1192.abstract.
[5] D. Resnik, D. Vrtačnik, M. Možek, B. Pečar, S. Amon, Experimental study of heat-treated thin film Ti/Pt heater and temperature sensor properties on a Si microfluidic platform, J. Micromech. Microeng. 21 (2011), http://dx.doi.org/10.1088/0960-1317/21/2/025025.
[6] G. Bernhardt, C. Silvestre, N. Le Cursi, S.C. Moulzolf, D.J. Frankel, R.J. Lad, Performance of Zr and Ti adhesion layers for bonding of platinum metallization to sapphire substrates, Sensors Actuators, B Chem. 77 (2001) 368–374, http://dx.doi.org/10.1016/S0925-4005(01)00756-0.
[7] G.-S. Chung, J.-M. Jeong, Fabrication of micro heaters on polycrystalline 3C-SiC suspended membranes for gas sensors and their characteristics, Microelectron. Eng. 87 (2010) 2348–2352.
[8] R.M. Tiggelaar, J.W. Berenschot, J.H. De Boer, R.G.P. Sanders, J.G.E. Gardeniers, R.E. Oosterbroek, A. Van Den Berg, M.C. Elwenspoek, Fabrication and characterization of high-temperature microreactors with thin film heater and sensor patterns in silicon nitride tubes, Lab Chip 5 (2005) 326–336, http://dx.doi.org/10.1039/b414857f.
[9] R. Srinivasan, I. Hsing, P.E. Berger, K.F. Jensen, S.L. Firebaugh, M.A. Schmidt, M.P. Harold, J.J. Lerou, J.F. Ryley, Micromachined reactors for catalytic partial oxidation reactions, AIChE J. 43 (1997) 3059–3069.
[10] M. Islam, T. Purtonen, H. Piili, A. Salminen, O. Nyrhilä, Temperature profile and imaging analysis of laser additive manufacturing of stainless steel, Phys. Procedia. 41 (2013) 835–842.
[11] D. Hu, R. Kovacevic, Modelling and measuring the thermal behaviour of the molten pool in closed-loop controlled laser-based additive manufacturing, Proc. Inst. Mech. Eng. Part B J. Eng. Manuf. 217 (2003) 441–452.
[12] B. Yuan, G.M. Guss, A.C. Wilson, S.P. Hau-Riege, P.J. DePond, S. McMains, M.J. Matthews, B. Giera, Machine-learning-Based monitoring of laser powder bed fusion, Int. J. Adv. Mater. Technol. 3 (2018), 1800136.
[13] H. Exner, M. Horn, A. Streek, F. Ullmann, L. Hartwig, P. Regenfuß, R. Ebert, Laser micro sintering: a new method to generate metal and ceramic parts of high resolution with sub-micrometer powder, Virtual Phys. Prototyp. 3 (2008) 3–11.
[14] B. Nie, L. Yang, H. Huang, S. Bai, P. Wan, J. Liu, Femtosecond laser additive manufacturing of iron and tungsten parts, Appl. Phys. A. 119 (2015) 1075–1080.
[15] S. Han, S. Hong, J. Ham, J. Yeo, J. Lee, B. Kang, P. Lee, J. Kwon, S.S. Lee, M. Yang, Fast plasmonic laser nanowelding for a Cu-Nanowire percolation network for flexible transparent conductors and stretchable electronics, Adv. Mater. 26 (2014) 5808–5814.
[16] D. Paeng, J. Yoo, J. Yeo, D. Lee, E. Kim, S.H. Ko, C.P. Grigoropoulos, Low-cost facile fabrication of flexible transparent copper electrodes by nanosecond laser ablation, Adv. Mater. 27 (2015) 2762–2767.
[17] L. Wang, Y. Rho, W. Shou, S. Hong, K. Kato, M. Eliceiri, M. Shi, C.P. Grigoropoulos, H. Pan, C. Carraro, D. Qi, Programming nanoparticles in multiscale: optically modulated assembly and phase switching of silicon nanoparticle array, ACS Nano 12 (2018) 2231–2241, http://dx.doi.org/10.1021/acsnano.8b00198.
[18] D. Qi, S. Tang, L. Wang, S. Dai, X. Shen, C. Wang, S. Chen, Pulse laser-induced size-controllable and symmetrical ordering of single-crystal Si islands, Nanoscale 10 (2018) 8133–8138, http://dx.doi.org/10.1039/C8NR00210J.
[19] D. Qi, D. Paeng, J. Yeo, E. Kim, L. Wang, S. Chen, C.P. Grigoropoulos, Time-resolved analysis of thickness-dependent dewetting and ablation of silver films upon nanosecond laser irradiation, Appl. Phys. Lett. 108 (2016), 211602, http://dx.doi.org/10.1063/1.4952597.
[20] J. Long, P. Fan, M. Zhong, H. Zhang, Y. Xie, C. Lin, Superhydrophobic and colorful copper surfaces fabricated by picosecond laser induced periodic nanostructures, Appl. Surf. Sci. 311 (2014) 461–467.
[21] C.W. Chang, D. Okawa, A. Majumder, A. Zettl, Solid-state thermal rectifier, Science 314 (2006) 1121–1124, http://dx.doi.org/10.1126/science.1132898.
[22] R. Vargas, T. Goto, W. Zhang, T. Hirai, Epitaxial growth of iridium and platinum films on sapphire by metalorganic chemical vapor deposition, Appl. Phys. Lett. 65 (1994) 1094–1096, http://dx.doi.org/10.1063/1.112108.
[23] R.W. Powell, C.Y. Ho, P.E. Liley, Thermal Conductivity of Selected Materials, US Department of Commerce, National Bureau of Standards Washington, DC, 1966.
[24] D.R. Lide, CRC Handbook of Chemistry and Physics, CRC, Boca Raton, 2012.
[25] C.Y. Ho, R.E. Taylor, Thermal expansion of solids, ASM International, 1998.
[26] Goodfellow, Titanium Dioxide-Titania(TiO_2), AZoM. (2018). doi:https://www.azom.com/properties.aspx?ArticleID=1179.
[27] B. Gliniecki, Platinum temperature sensor technology, Trend Watch Mater. Asembly (2013), T5 https://www.heraeus.com/media/media/group/doc_group/products_1/hst/usa_only/technical_articles/DesignNews.pdf.
[28] A. Wang, L. Jiang, X. Li, Y. Liu, X. Dong, L. Qu, X. Duan, Y. Lu, Mask-free patterning of high-conductivity metal nanowires in open air by spatially modulated femtosecond laser pulses, Adv. Mater. 27 (2015) 6238–6243, http://dx.doi.org/10.1002/adma.201503289.
[29] Y. Nakajima, K. Obata, M. Machida, A. Hohnholz, J. Koch, O. Suttmann, M. Terakawa, Femtosecond-laser-based fabrication of metal/PDMS composite microstructures for mechanical force sensing, Opt. Mater. Express 7 (2017) 4203, http://dx.doi.org/10.1364/OME.7.004203.
[30] Q. Chen, T. Tong, J.P. Longtin, S. Tankiewicz, S. Sampath, R.J. Gambino, Novel sensor fabrication using direct-write thermal spray and precision laser micromachining, J. Manuf. Sci. Eng. Asme. 126 (2004) 830–836, http://dx.doi.org/10.1115/1.1813481.
[31] S. Hong, J. Yeo, W. Manorotkul, G. Kim, J. Kwon, K. An, S.H. Ko, Low-temperature rapid fabrication of ZnO nanowire UV sensor array by laser-induced local hydrothermal growth, J. Nanomater. 2013 (2013) 2.
[32] M. Brandt, The Role of Lasers in Additive Manufacturing, Elsevier Ltd, 2016, http://dx.doi.org/10.1016/B978-0-08-100433-3.02001-7.
[34] S.L. Firebaugh, K.F. Jensen, M.A. Schmidt, Investigation of high-temperature degradation of platinum thin films with an in situ resistance measurement apparatus, J. Microelectromech. Syst. 7 (1998) 128–135, http://dx.doi.org/10.1109/84.661395.
[35] M. Wada, T. Maeda, S. Inoue, Single crystal level high temperature coefficient of resistance for a platinum thin film on a sapphire substrate by thermal treatment, J. Japan Inst. Met. Mater. 76 (2012) 359–363, http://dx.doi.org/10.2320/jinstmet.76.359.
[36] A. Ababneh, A.N. Al-Omari, A.M.K. Dagamseh, M. Tantawi, C. Pauly, F. Mücklich, D. Feili, H. Seidel, Electrical and morphological characterization of platinum thin-films with various adhesion layers for high temperature applications, Microsyst. Technol. 23 (2017) 703–709, http://dx.doi.org/10.1007/s00542-015-2715-0.
[37] V. Guarnieri, L. Biazi, R. Marchiori, A. Lago, Platinum metallization for MEMS application. Focus on coating adhesion for biomedical applications, Biomatter. 4 (2014), e28822, http://dx.doi.org/10.4161/biom.28822.
[38] S. Halder, T. Schneller, R. Waser, Enhanced stability of platinized silicon substrates using an unconventional adhesion layer deposited by CSD for high temperature dielectric thin film deposition, Appl. Phys. A Mater. Sci. Process. 87 (2007) 705–708, http://dx.doi.org/10.1007/s00339-007-3866-3.
[39] A. Ababneh, A.N. Al-Omari, M. Marschibois, D. Feili, H. Seidel, Investigations on the high temperature compatibility of various adhesion layers for platinum, Proc. SPIE. Int. Soc. Opt. Eng. 8763 (2013), 87631Z, http://dx.doi.org/10.1117/12.2017333.
[40] W. Sripumkhai, S. Porntheeraphat, B. Saekow, W. Bunjongpru, S. Rahong, J. Nukeaw, Effect of annealing temperature on platinum thin films prepared by Electron beam evaporation, J. Microsc. Soc. Thail. 24 (2010) 51–54.

[41] G. Fischer, H. Hoffmann, J. Vancea, Mean free path and density of conductance electrons in platinum determined by the size effect in extremely thin films, Phys. Rev. B 22 (1980) 6065.
[42] U. Schmid, H. Seidel, Influence of thermal annealing on the resistivity of titanium/platinum thin films, J. Vac. Sci. Technol. A 24 (2006) 2139–2146, http://dx.doi.org/10.1116/1.2359739.
[43] F.N. Mohamed, M.S.A. Rahim, N. Nayan, M.K. Ahmad, M.Z. Sahdan, J. Lias, Influence of TiO2 Thin Film Annealing Temperature on Electrical Properties Synthesized by CVD Technique, 2015.
[44] J. Li, S. Chen, D. Qi, W. Huang, C. Li, H. Lai, Energy band design for p-type tensile strained Si/SiGe multi-quantum well infrared photodetector, Optoelectron. Lett. 7 (2011) 175–177.
[45] S. Heo, S. Baek, D. Lee, M. Hasan, H. Jung, J. Lee, H. Hwang, Sub-15 nm n+/p-Germanium shallow junction formed by PH3 plasma doping and excimer laser annealing, Electrochem. Solid-State Lett. 9 (2006), G136–G137.
[46] D. Qi, H. Liu, W. Gao, S. Chen, C. Li, H. Lai, W. Huang, J. Li, Investigations of morphology and formation mechanism of laser-induced annular/droplet-like structures on SiGe film, Opt. Express 21 (2013) 9923–9930, http://dx.doi.org/10.1364/OE.21.009923.
[47] J. Han, P. Cheng, H. Wang, C. Zhang, J. Zhang, Y. Wang, L. Duan, G. Ding, MEMS-based Pt film temperature sensor on an alumina substrate, Mater. Lett. 125 (2014) 224–226, http://dx.doi.org/10.1016/j.matlet.2014.03.170.
[48] R.M. Tiggelaar, R.G.P. Sanders, A.W. Groenland, J.G.E. Gardeniers, Stability of thin platinum films implemented in high-temperature microdevices, Sens. Actuators, A Phys. 152 (2009) 39–47, http://dx.doi.org/10.1016/j.sna.2009.03.017.
[49] V.N. Kuznetsov, N. Serpone, Visible light absorption by various titanium dioxide specimens, J. Phys. Chem. B 110 (2006) 25203–25209, http://dx.doi.org/10.1021/jp064253b.
[50] A. Yildiz, S.B. Lisesivdin, M. Kasap, D. Mardare, Electrical properties of TiO2 thin films, J. Non. Solids 354 (2008) 4944–4947, http://dx.doi.org/10.1016/j.jnoncrysol.2008.07.009.
[51] W.A. Strifler, C.W. Bates, Stress in evaporated films used in GaAs processing, J. Mater. Res. (1991).
[52] M. Hatano, S. Moon, M. Lee, K. Suzuki, C.P. Grigoropoulos, In situ and ex situ diagnostics on melting and resolidification dynamics of amorphous and polycrystalline silicon thin films during excimer laser annealing, J. Non. Solids 266–269 (2000) 654–658, http://dx.doi.org/10.1016/S0022-3093(99)00768-1.
[53] D.P. Brunco, J. a Kittl, M. Thompson, Time-resolved temperature measurements using thin film metal thermometers, Rev. Sci. Instrum. 64 (1993) 2615–2623.
[54] S. Haas, G. Schöpe, C. Zahren, H. Stiebig, Analysis of the laser ablation processes for thin-film silicon solar cells, Appl. Phys. A Mater. Sci. Process. 92 (2008) 755–759, http://dx.doi.org/10.1007/s00339-008-4560-9.
[55] P. Lorenz, T. Smausz, T. Csizmadia, M. Ehrhardt, K. Zimmer, B. Hopp, Shadowgraph studies of laser-assisted non-thermal structuring of thin layers on flexible substrates by shock-wave-induced delamination processes, Appl. Surf. Sci. 336 (2015) 43–47, http://dx.doi.org/10.1016/j.apsusc.2014.09.114.

Biographies

Letian Wang received his B. Sci. in 2014 from Department of Thermal Engineering, Tsinghua University, China. He is currently a Ph.D. candidate in Laser Thermal Lab, Department of Mechanical Engineering, UC Berkeley. His research interests lie in laser processing of semiconductor nanostructure, ultrafast probing and diagnostics and manufacturing process control.

Zeqing Jin received his B. Sci. from Mechanical Engineering from University of Michigan-Shanghai JiaoTong University, Joint Institute, China. He is currently a master student major in Mechanical Engineering at University of Rochester and a visiting researcher at University of California, Berkeley. His research interests focus on ultrafast laser fabrication, computer vision and artificial intelligence powered additive manufacturing.

Dongwoo Paeng received his Ph.D. in 2016 from Department of Mechanical Engineering, UC Berkeley, USA. He is currently at Lam Research, USA as a process engineer. His research interest lies in laser processing of semiconductor, electro magnetic wave, thermal simulation and manufacturing equipment design.

Yoonsoo Rho is a Ph.D. candidate in Laser Thermal Lab, Department of Mechanical Engineering, UC Berkeley, USA. He received his B. Sci. in 2010 from Department of Mechanical Engineering, Korea Advanced Institute of Technology, South Korea. His main research focus on the laser processing of two-dimensional materials and multiphoton based near-filed scanning optical microscopy (NSOM).

Jiangyou Long received his B.E. degree in 2012 and Ph.D. degree in 2017 from Tsinghua University. He is now a postdoctoral researcher in Laser Thermal Laboratory, UC Berkeley. His current research focuses on liquid-assisted laser materials processing.

Matthew Eliceiri received his Bachelor of Science from UC Berkeley in May 2019 and is currently a mechanical engineering PhD student in the laser thermal lab at UC Berkeley. His research interests lie in laser ablation imaging and diagnostics, and in ultrafast pump and probe techniques in semiconducting materials.

YS Kim brings 28 years of semiconductor experience on the process and hardware development in clean, etch, and CVD area of semiconductor manufacturing. He has developed and launched many different processes and products such as MERIE, Helicon ICP, dual station HF plasma etch, Bevel etch & dep, and Backside dep, etc. YS has worked at Lam Research for 16 years after 10 years in Applied Materials and 5 years in Plasma Materials Technology, respectively. Mr. Kim holds a MS in Material Science.

Costas P. Grigoropoulos is A. Martin Berlin Chair Professor in the Department of Mechanical Engineering at UC Berkeley. He received his Diploma Degrees in the National Technical University of Athens, Greece. He holds a Ph.D. in Mechanical Engineering from Columbia University. He is a Fellow of ASME and SPIE and an Editor for the International Journal of Heat and Mass Transfer. His current research interests are in laser materials processing for electronics manufacturing, laser-aided fabrication of flexible devices, energy systems and biomaterials, the study of ultrafast laser-matter interaction, fundamental microscale transport, the design and fabrication of architected mechanical materials.